

Trions, excitons, and scattering states in multiple quantum wells with a variable-concentration electron gas

R. T. Cox

Equipe Nanophysique et Semiconducteurs, Service de Physique des Matériaux et Microstructures, CEA-Grenoble, 38054 Grenoble, France

R. B. Miller

Department of Physics, La Trobe University, Victoria 3086, Australia

K. Saminadayar

Université Joseph Fourier de Grenoble and Equipe Nanophysique et Semiconducteurs, Service de Physique des Matériaux et Microstructures, CEA-Grenoble, 38054 Grenoble, France

T. Baron

Laboratoire des Technologies de la Microélectronique, UMR 5129 CNRS/CEA-Grenoble, 38054 Grenoble, France

(Received 7 December 2003; published 3 June 2004)

CdTe/Cd_{1-x}Zn_xTe multiple quantum wells were modulation doped with indium donors compensated by nitrogen acceptors so that the two-dimensional electron concentration in the wells (n_e) could be varied from near 0 up to $\approx 10^{11}$ cm⁻² by optical pumping. In zero field at $T=2$ K, the optical absorption spectra show trion (X^-) and exciton (X) resonance peaks at low n_e , with an electron-exciton scattering wing extending to high energy from the exciton resonance. At the highest n_e , the spectrum evolves towards the single asymmetric peak traditionally associated with the many-body “Fermi edge singularity” but its total integrated intensity remains almost constant, in agreement with recent few-body theories of the optical response at $n_e \ll 1/a_B^2$. Under magnetic field $B=8$ T at $T=2$ K, sharp X^- and X resonance peaks are seen as well as a broad band Z situated about $\hbar\omega_{ce}$ (the electron cyclotron energy) higher in energy. Band Z is attributed to a known exciton-electron scattering process [Yakovlev *et al.*, Phys. Rev. Lett. **79**, 3974 (1997)] where the electrons are magnetically quantized. In σ^+ circular polarization, the X resonance attenuates rapidly with n_e but the X^- resonance grows almost as rapidly (“intensity sharing”) so that their intensity sum falls only slowly. In σ^- the X resonance also attenuates rapidly with n_e and the Z band grows to compensate, with the intensity sum again falling only slowly. It is concluded that the spectrum evolution as n_e varies from 0 to 10^{11} cm⁻² in CdTe is due to intensity sharing between the X and X^- resonances and between these resonances and scattering processes. This is a low n_e (and low B) model of the excitonic properties, where screening and phase-space filling contribute only to the $<10\%$ decrease of the oscillator strength sums. As regards the samples’ luminescence properties, two series of phonon peaks seen in emission spectra are attributed to recombination of two-dimensional electrons with nitrogen acceptors that have migrated close to and into the wells.

DOI: 10.1103/PhysRevB.69.235303

PACS number(s): 78.67.De, 78.30.Fs, 78.40.Fy, 78.55.Et

I. INTRODUCTION

In optical studies of semiconductor quantum wells containing a two-dimensional electron gas, the electron concentration per unit area (n_e) is naturally a principal experimental parameter. It is therefore very helpful to have a method of varying n_e in a given sample, rather than use a set of samples each with different doping levels.

Most frequently, n_e is controlled in modulation-doped single quantum well structures by applying a depleting voltage to a transparent Schottky gate deposited on the sample surface.¹⁻⁴ However, surface gating is not appropriate for a multiple quantum well (MQW) sample, as the multiple wells at successively greater depths will not deplete together.

But studies of MQW’s rather than single quantum wells can be very useful, especially for absorption spectroscopy where the weak responses of the individual wells will add up to give more accurately measurable values. And absorption spectroscopy is fundamental because (compared to photolu-

minescence excitation or photocurrent spectroscopies) it gives absolute values for the oscillator strengths of excitonic resonances and other optical processes.

Hence we have been working on MQW structures where the electron concentration could be varied in all the wells together by an optical pumping method. Our samples are CdTe quantum wells separated by Cd_{1-x}Zn_xTe barriers. The structures are modulation doped in the usual way with donor impurities (indium) in the barriers. But we compensate the donors with acceptor impurities (nitrogen), also doped into the barriers, so that ideally $n_e \approx 0$ in the quantum wells in thermal equilibrium. Under illumination with light above the barrier band gap, free electrons accumulate in the CdTe wells while the corresponding holes become trapped at the acceptors in the CdZnTe barriers.

As illustrated in Fig. 1, the holes get trapped because the valence-band offset is very small at a CdTe/CdZnTe interface: The barrier acceptors make a deeper hole trap than the valence-band wells. The excess electron concentration in the

wells, n_e , increases with the illumination intensity. In a sense, illumination “uncompensates” the sample and the ultimate limit of n_e is fixed (as in conventional, single-impurity modulation doping) by the barrier donor concentration.

The 2 K spectra of the CdTe wells modified by the presence of the electron gas show absorption/emission peaks associated with the creation/annihilation transitions of neutral excitons X and of charged excitons (trions) X^- . The spectra also show very strong electron-acceptor recombination peaks in emission.

The present paper completes a previous brief report on these double-doped samples.⁵ It also corrects several of our previous conclusions, in the light of recent progress in the theory of the optical response of a 2D semiconductor with a dilute electron gas.^{6–9} Here, dilute means $n_e \ll 1/a_B^2$, that is, $n_e \ll 2 \times 10^{12} \text{ cm}^{-2}$ (where a_B is the excitonic Bohr radius = 7 nm in bulk CdTe).

Sections II and III present the experimental methods and sample characterization. We then give absorption spectra as a function of n_e , in zero field (Sec. IV A) and under applied magnetic field B to 8 T (Sec. IV B). Especially, we measure properties of the exciton and trion-creation transitions, and also of electron-exciton scattering processes, both at $B=0$ and $B=8$ T.

The data are analyzed in Sec. V. In Sec. V A (zero-field spectra), we find that the oscillator strength associated with the excitonic resonance is transferred progressively to exciton-electron scattering and trion-creation transitions as n_e increases, with the total intensity integrated over all processes remaining surprisingly stable.

In Secs. V B and V C (analysis of magnetoabsorption), we attempt to demonstrate that there is no fundamental change in this pattern of oscillator-strength sharing at $B=8$ T. Even as the lowest spin sublevel of the lowest conduction-band Landau level fills with electrons up towards filling factor $\nu = 1$, it appears unnecessary to invoke any large contribution of phase-space filling or screening effects to explain the observed strong weakening of the excitonic resonance, at least in CdTe QW's with n_e of order 10^{11} cm^{-2} .

But with the two-dimensional (2D) electron-gas spin polarized, the optical spectrum is very different in the two circular polarizations. In σ^+ polarization, the X resonance shares intensity out mainly to the trion resonance X^- as n_e increases. In σ^- it shares intensity out to a broad peak Z which we attribute to the magnetically quantized exciton-electron scattering process identified by Yakovlev *et al.*¹⁰ As in zero field, the total intensity integrated over all three processes shows only a small decrease with n_e .

II. EXPERIMENT

Samples are ten-period CdTe/Cd_{1-x}Zn_xTe ($x = 0.13-0.14$) multiple quantum wells grown by molecular-beam epitaxy with their average lattice matched to [100] orientation Cd_{1-x}Zn_xTe ($x = 0.12$) substrates. The CdTe wells are 10 nm thick and the CdZnTe barrier thickness is 80 nm.

The growth temperature was 220 °C, well below the optimum for growing good interfaces but chosen to reduce seg-

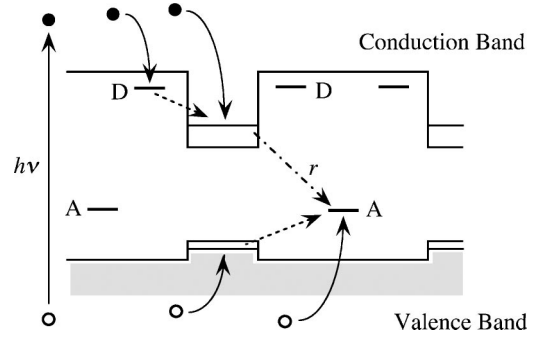


FIG. 1. Optically induced charge separation process in our CdTe/CdZnTe MQW's with compensated donor and acceptor dopings in the barriers. The pumping light $h\nu$ generates free electrons and holes. Electrons collect in the deep conduction-band wells. Holes get trapped at acceptors because the valence-band well is shallower than the 55 meV barrier acceptor levels. Competition between electron-acceptor tunneling recombination (r) and optical pumping ($h\nu$) determines n_e .

regation and diffusion of the dopants. As schematized in Fig. 1, we introduced planes of indium donors in the barriers at 25 nm from the well edges (two planes per period, each nominally $5 \times 10^{10} \text{ In cm}^{-2}$). A nominally single plane of acceptors was introduced at each barrier center, that is, at 40 nm from the well edges.

In fact, even at 220 °C, nitrogen dopant unfortunately undergoes considerable movement, towards and even into the wells, see also Ref. 11. This led to fast electron-acceptor recombination rates, so that we had to use high pumping powers to achieve the desired values of n_e . (This is unlike the relatively easy control of hole concentration in p -type CdTe/CdMgTe single QWs, see, e.g. Ref. 12, which works via charge transfer to natural depletion states localized on the CdMgTe surface.)

Also, since the efficiency of nitrogen doping is very low ($\approx 10^{-3}$ only) in CdTe and in low zinc content CdZnTe alloys,¹³ it proved very hard to adjust the nitrogen concentration accurately. Sample type (n or p) was determined by capacitance-voltage ($C-V$) measurements. Our intention was to compensate 10^{11} donors cm^{-2} per period exactly, by introducing 10^{11} acceptors cm^{-2} per period. Of five samples grown, S1 . . . S5, fairly close compensation was achieved with two samples S3 and S5.

Absorption in the quantum well exciton range starting at ≈ 1.60 eV was measured with a tungsten lamp as light source, with the samples at 2 K in pumped helium. The Cd_{0.88}Zn_{0.12}Te substrates with optical cutoff at 1.66 eV are transparent in the quantum well exciton region, but they filter out all the above barrier-band-gap light from the lamp; this we call absorption measurements “in the dark.”

To pump electrons into the quantum wells, we used a titanium sapphire laser beam at 710 nm (1.75 eV), just above the Cd_{1-x}Zn_xTe ($x = 0.135$) barrier band gap. The beam spot size was 1 mm, giving fairly uniform coverage of a 0.5 mm diameter aperture on the front of the sample. The pump laser induced luminescence (very strong at high powers), so the pure absorption spectrum was extracted by taking the difference between transmission spectra with and without the

tungsten lamp. At the highest powers used (≈ 100 mW over 1 mm diameter), the helium was starting to boil at the sample surface.

The transmission of the MQW drops to 0.1 or less in the main exciton and trion absorption peaks. Spectra were converted to optical density by taking $\log_{10}(1/\text{transmission})$. Reflection corrections were not needed for these ten-period structures.

Only 10% of the red pumping light reaches to the full depth of the $0.9 \mu\text{m}$ thick sample and, in retrospect, it might have been better to grow a smaller number of periods. However, photocarriers can diffuse distances of order $1 \mu\text{m}$, and the $\log(\text{power})$ dependence of n_e (see below) helps reduce any concentration gradient. We found no obvious indication in our spectra for different values of n_e in the ten wells.

Assuming equality between the wells, we can attempt to predict the dependence of n_e on pumping power, referring to the analysis¹⁴ of photoeffects in modulation doped GaAs/GaAlAs heterojunctions having unintentional deep acceptors in the GaAlAs layer.

The photoinduced transfer of negative charge from A^- centers to the QW's is limited, at low T , by tunneling assisted electron-acceptor recombination (Fig. 1). Electrons confined in levels at energy E in the QW's tunnel through potential barriers of height profile $\Delta V(x)$ (measured with respect to E) to recombine with acceptors at distance d . The WKB tunneling probability is $e^{-2\gamma}$ with $\gamma = (1/\hbar) \int_0^d \sqrt{2m_e e \Delta V} dx$. At equilibrium in a plane of acceptors at distance d , the annihilation rate, which is $\propto n_e n_{A^0} [(\sqrt{\Delta V})_{\text{mean}} d]$, is equal to the hole trapping rate, which is $\propto n_{A^-} \times$ pumping power.

The equilibrium equation is complicated because the barrier profile $\Delta V(x)$ depends self-consistently on n_e (the barriers become more transparent as negative charge is added to the wells). The n_e dependence of the tunneling exponents -2γ dominates in determining the n_e dependence of the rate equations, except near the minimum and maximum values of n_e . Then, the electron-acceptor recombination rate tends to increase exponentially with n_e , because the average square-root barrier profile $(\sqrt{\Delta V})_{\text{mean}}$ decreases with n_e^p , with p not much less than 1.0 for our sample geometry.

So the pumping rate necessary to equilibrate tunneling recombination is approximately an exponential function of n_e . In other words we expect n_e to be approximately proportional to $\log(\text{pump power})$, except near the initial and saturation values.

In Sec. V we will use $\log(\text{pump power})$ as abscissa to graph spectrum properties. This concentration scale should be considered as indicative only. However, the measured intensity of the high-field trion resonance (Sec. V B), which provides an alternate scale, is consistent with an approximately logarithmic power dependence of n_e .

III. EMISSION SPECTRA

We begin by discussing $S1$, the first sample grown, which had too much nitrogen: It was p -type electrically, with hole concentration $p \approx 2.0 \times 10^{11} \text{ cm}^{-2}$ per period. Even under

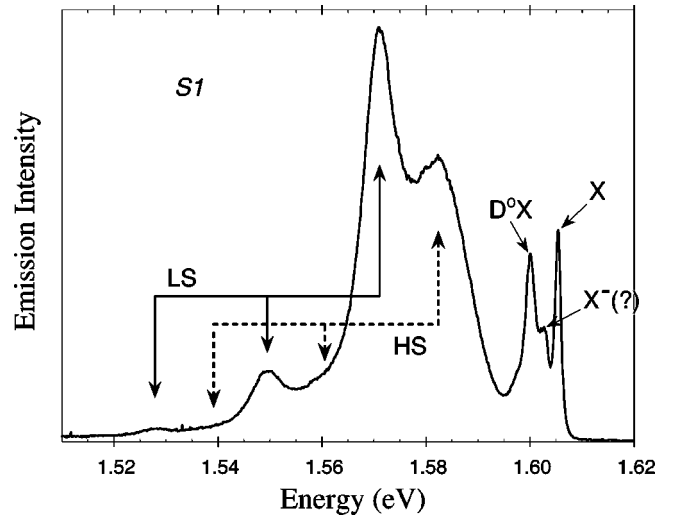


FIG. 2. Emission spectrum of N and In doped CdTe/CdZnTe MQW sample $S1$ excited by blue argon laser light at 2 K, showing excitonic peaks at 1.60–1.61 eV and the “higher series” (HS) and “lower series” (LS) of electron to acceptor recombination peaks.

very strong optical pumping, the threshold region of its absorption spectrum showed no trion peak, only the neutral $1s$ exciton peak (X) and a weak donor-bound exciton peak (D^0X). Observation of neutral donors D^0 in the wells implies very low free-electron concentration (otherwise one would have charged donors D^-).

The nature of its luminescence spectrum, see Fig. 2, helped us to understand why n_e remained so low for sample $S1$. In the quantum well band-gap region, we identify heavy-hole X and D^0X peaks, possibly a trion peak (X^-), but the dominant emission consists of intense, broad peaks at lower energy.

One can distinguish two series of peaks: a “lower series” (LS) and a “higher series” (HS). The individual members of each series are separated by the LO phonon energy of 21 meV. In CdTe, strong phonon replicas are characteristic of annihilation of a localized hole. We attribute these peaks to electron-acceptor recombination $e^- + A^0 \rightarrow A^- + \hbar\omega$, a recombination process that is normally undetectable in undoped CdTe/CdZnTe quantum well structures.

Our identification of these transitions lies outside the main theme of this paper and is presented in the Appendix. The recombining electrons are in the E1 subbands of the quantum wells. The acceptors are the nitrogen dopant atoms, situated in the quantum wells for the LS peaks, in the barriers near the QW edges for the HS peaks (see the Appendix).

So recombination with a large excess of neutral nitrogen acceptors situated in and near the wells (implying massive migration of the nitrogen dopant deposited at the barrier centers) was preventing buildup of free electrons in sample $S1$. Therefore, we grew further samples with progressively lower nitrogen doses. Sample $S2$ still had far too much nitrogen but sample $S3$, although still slightly p type in C - V measurements ($p \approx 3 \times 10^{10} \text{ cm}^{-2}$ per period) proved almost optimum for our studies. The final samples had somewhat too little nitrogen and were n type: Sample $S4$ had $n \approx 1 \times 10^{11} \text{ cm}^{-2}$ and sample $S5$ had $n \approx 3 \times 10^{10} \text{ cm}^{-2}$ per pe-

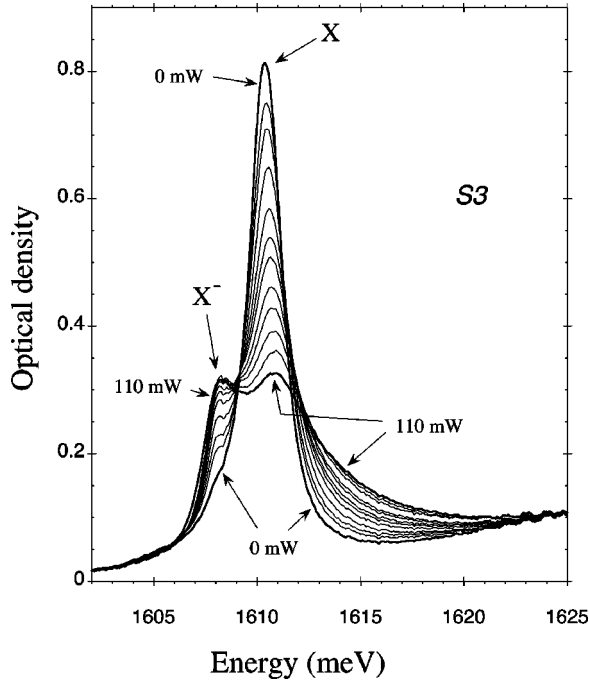


FIG. 3. Optical density $\log_{10}(1/t)$ of CdTe/CdZnTe MQW sample *S3* at $B=0$, nominal $T=2$ K, for various pump powers, showing increase of trion absorption peak and decrease and asymmetric broadening of exciton peak with increasing n_e .

riod, as determined from the room temperature C - V measurements. These numbers become $n = 1.1 \times 10^{11} \text{ cm}^{-2}$ and $n \approx 4 \times 10^{10} \text{ cm}^{-2}$, respectively, when determined from the 2 K magneto-optics studies in the dark (Secs. IV B and V B).

Samples *S3*, *S4*, and *S5* still gave intense electron-acceptor recombination bands but, significantly, the trion recombination peak (considerably broadened for sample *S5*) dominated the excitonic region of their emission spectra.

IV. ABSORPTION SPECTRA

A. Zero-field spectra

Figure 3 shows an overlaid set of optical density spectra for different laser pumping powers for sample *S3* in zero magnetic field. (The upward slope of the base line from left to right is due to the low-energy tail of the substrate's band-gap absorption; the weak oscillations starting at 1621 meV are gaseous oxygen bands.)

In the dark (zero pump power), we have an intense heavy-hole exciton peak (X) about 2 meV wide and a very weak heavy-hole trion peak (X^-) in its low-energy wing. These peaks correspond to the two fundamental optical processes

$$\hbar\omega_X \rightarrow X, \quad (1a)$$

$$\hbar\omega_T + e^- \rightarrow X^-, \quad (1b)$$

respectively. (The weak X^- peak may be due to electrons induced by stray light at low T since sample *S3* measured slightly p type electrically at room T .)

Note that light-hole excitons are not seen for these samples due to the large strain splitting imposed on the CdTe

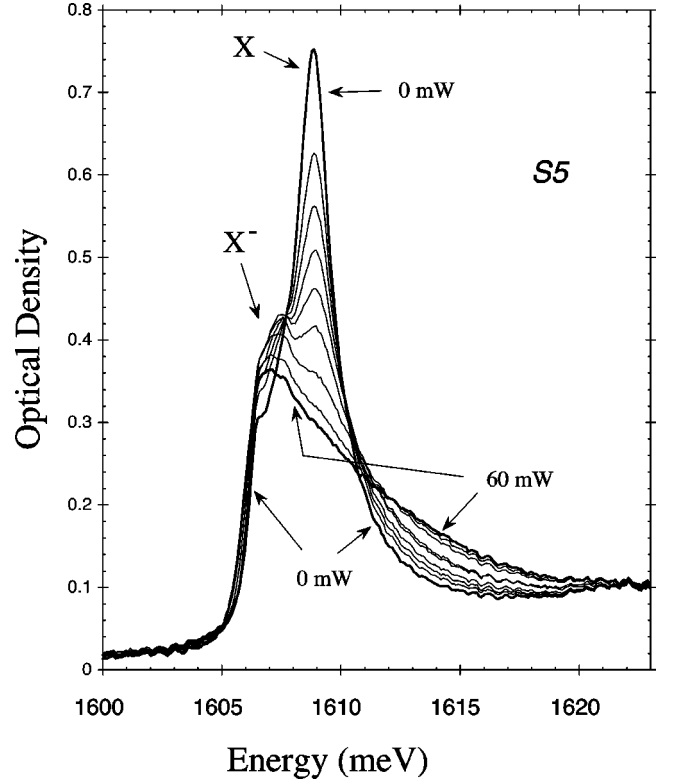


FIG. 4. Optical density $\log_{10}(1/t)$ of sample *S5* at $B=0$, nominal $T=2$ K for various pump powers, showing evolution of trion peak to “Fermi edge singularity-like” form.

QW valence band by Cd_{0.88}Zn_{0.12}Te substrates.¹⁵ This considerably simplifies our spectra and their analysis, particularly under magnetic field.

Figure 3 shows very clearly the remarkable evolution of the exciton and trion peaks with increasing n_e . As we increase the pumping power, the excitonic absorption broadens and its peak amplitude decreases. The broadening is asymmetric towards the high-energy side. Such broadening has been explained in terms of many-body processes^{16–20} or (more recently) just three-body processes,^{7–9,21} where background electrons are excited to higher energy states during the exciton creation event.

Simultaneously, the X^- absorption peak gains intensity and has become a very significant feature in the spectrum at the highest pump power (110 mW). Comparing to spectra of other samples with known (fixed) n_e , we estimate that the 110 mW spectrum corresponds to $n_e \approx 6 \times 10^{10} \text{ cm}^{-2}$.

Figure 4 shows further evolution of the absorption spectrum, for the slightly n -type sample *S5* which starts from a higher initial value of n_e in the dark. The trion absorption evolves to a form that looks like the classical, asymmetric “Fermi edge singularity” (FES) and the exciton peak is lost in the high-energy wing. For the highest pump power (60 mW) in Fig. 4, we estimated $n_e = 9.2 \times 10^{10} \text{ cm}^{-2}$ from detecting the onset of emptying of the lowest free-electron Landau level at $B = 1.9$ T (see Sec. IV B).

The more strongly n -type sample *S4* already gives this kind of FES-like absorption shape in the dark (see its zero-field spectrum at bottom right in Fig. 5). Its electron concen-

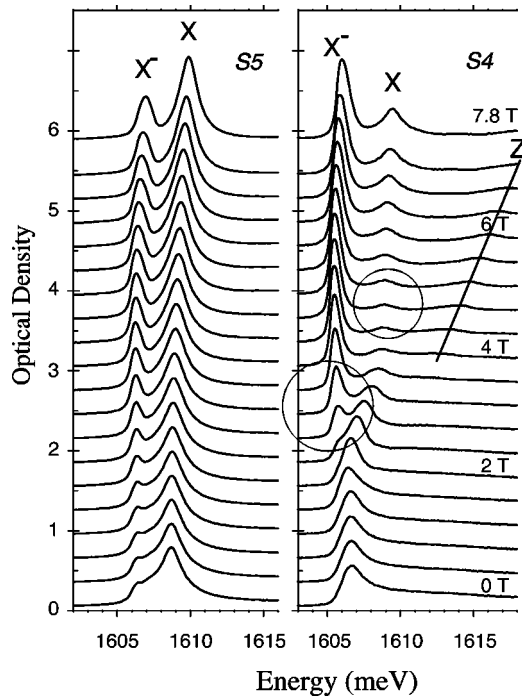


FIG. 5. Stacked absorption spectra for CdTe/CdZnTe MQW samples S5 and S4 in the dark at 2 K, in σ^+ polarization for various magnetic fields B . For S5 ($n_e \approx 4 \times 10^{10} \text{ cm}^{-2}$), distinct trion and exciton peaks are seen at all B from 0 to 7.8 T. Circled regions for sample S4 ($n_e = 1.1 \times 10^{11} \text{ cm}^{-2}$) show sharp trion resonance emerging from low-energy wing of the “FES-like” peak at 2.3 T ($\nu=2$), and exciton resonance emerging around 4.2 T. Sloping line marks field dependence of peak Z.

tration $n_e = 1.1 \times 10^{11} \text{ cm}^{-2}$ (also determined magneto-optically) appears almost saturated, increasing only a little under illumination, to $1.35 \times 10^{11} \text{ cm}^{-2}$.

B. Magnetoabsorption spectra

Even when the zero-field absorption spectrum has evolved to the broad FES-like form, a pair of sharp exciton and trion resonance peaks always reemerges at high enough magnetic field, at least for CdTe quantum wells.²² The sharp trion peak emerges first and a sharp exciton peak emerges later, at higher field.

The attribution of these sharp peaks to X and X^- is justified below (see after next paragraph). The fields B where they emerge have been associated^{22–24} with characteristic values of the Landau-level filling factor parameter $\nu = n_e h/eB$, which is sweeping down from infinity as B is swept upwards from 0. The X^- resonance emerges at $\nu = 2$, when the upper spin sublevel of the lowest Landau level $n=0$ begins to empty. The X resonance emerges at a less well-defined filling, perhaps varying with n_e and degree of disorder but usually somewhere around $\nu=1$ (where the lower spin sublevel of the $n=0$ Landau level starts to empty). These sharp peaks then persist to the highest fields available (e.g., 20 T in Ref. 24).

There has not been any real theory of this. The symmetric magnetoabsorption resonances X and X^- are somehow dif-

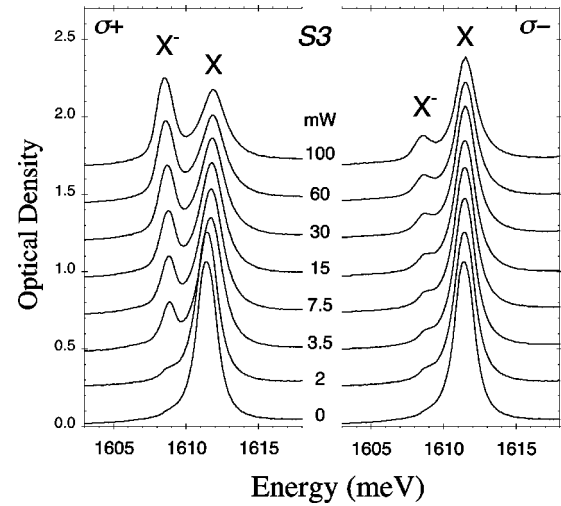


FIG. 6. Optical density of CdTe MQW sample S3 in σ^+ and σ^- polarizations at 8 T for various pump powers (nominal $T=2$ K), showing strengthening of the trion and weakening of the exciton as n_e increases up to $\approx 6 \times 10^{10} \text{ cm}^{-2}$.

ferent from the asymmetrically broadened zero-field excitations. This is presumably because the electronic continuum is quantized into Landau levels separated by the cyclotron energy $\hbar\omega_c$: The small amplitude excitations of the electron gas that broadened the exciton and trion asymmetrically at zero field no longer exist. But these excitations do persist as discrete “combined” exciton plus cyclotron processes¹⁰ and we will return to this point in Sec. V C.

That one can label the emerging magnetoabsorption peaks “trion” and “exciton” is confirmed by the continuity we see in resonance energy positions over the parameter space n_e, B for samples S3, S4, and S5. The pair of peaks resolved at all fields for low n_e correlates in position with the pair of peaks that are seen only at high fields for high n_e . We show this in Fig. 5 which compares field dependences in σ^+ polarization for samples S5 and S4, all the spectra being taken in the dark.

For sample S5 (with the lower n_e), trion and exciton absorption resonances are distinguished at all fields, including $B=0$. [See also, for example, the sets of reflectivity spectra for lightly modulation doped $\text{Cd}_{1-x}\text{Mn}_x\text{Te}$ ($x < 0.01$) QW’s given in Ref. 26.]

For sample S4 with higher n_e , which shows the FES-like spectrum form in zero field, narrow resonance X^- emerges at $B = 2.3$ T. Narrow resonance X emerges around 4.2 T.

These magnetoabsorption resonances have very different amplitudes in opposite circular polarizations, as seen for sample S3 at 8 T in Fig. 6 (but their Zeeman splitting, which varies with well width and strain state, is accidentally almost zero for these particular MQW’s.) As is well known, the trion absorption transition is strongly polarized σ^+ when the electrons become spin polarized at high B and low T ; this comes from the selection rules for the transition $\hbar\omega + e^- \rightarrow X^-$ that creates the electron-spin singlet trion, for the case of negative electron g factor g_e .²³ (We attribute the weak trion intensity seen in σ^- in Fig. 6 to electron spin depolarization by disorder, and also by sample heating at the higher pump powers.)

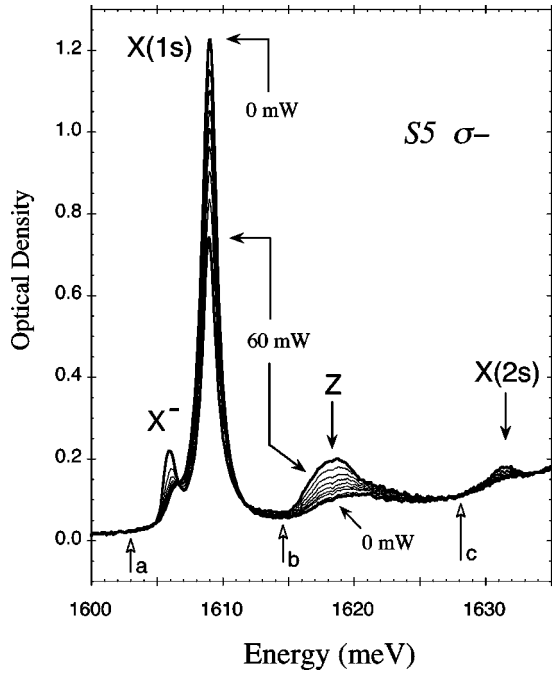


FIG. 7. Optical density of sample *S5* in σ^- polarization at $B = 8$ T, nominal $T = 2$ K, for pumping powers from 0 to 60 mW, showing weakening of 1s and 2s exciton peaks X and concurrent growth of absorption band Z as n_e increases. A weak trion peak X^- also appears due to spin depolarization. Arrows *a*, *b*, *c* mark integration ranges for Fig. 13.

We will be particularly concerned with the electron concentration dependence of the exciton peak's intensity, which has not previously been measured continuously over such a wide range at high field and has been variously interpreted. As seen in the σ^+ spectra of Fig. 6, the amplitude of the 1s exciton peak X at $B = 8$ T decreases considerably with increasing n_e .

The X peak's amplitude decreases less in the opposite polarization σ^- (see on the right in Fig. 6). This gives the σ^+ and σ^- spectra a complementary appearance, with the trion strong in σ^+ and the exciton strong in σ^- , see the 100 mW spectra in Fig. 6.

But an accurate analysis of the data (Sec. V B) will show that the strong polarization anisotropy seen for X is somewhat deceptive. It comes partly from an anisotropy in width and partly from a real but quite small inequality in the two quenching mechanisms that operate on σ^- and σ^+ excitons, respectively.

Figure 7 shows spectra extending out to higher energy, above the X^- and X resonances, for sample *S5* in σ^- polarization at $B = 8$ T.

Note first that this figure shows the 2s exciton at 1631.5 meV disappearing with increasing n_e . The beginning of this process can be seen in spectra (not shown here) for sample *S3* where the initial amplitude of the 2s exciton is several times larger. For sample *S4* with higher n_e the 2s exciton peak is no longer detectable. This behavior of the 2s exciton might be considered a paradox in some viewpoints.²⁵

But we will be concerned here with the broad absorption peak or band that we have labeled “Z” (to give it a neutral

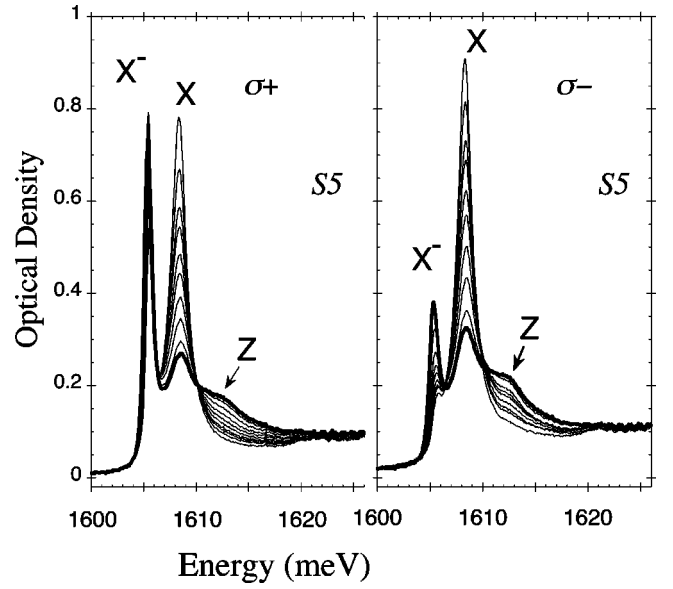


FIG. 8. Optical density of sample *S5* in σ^+ and σ^- polarizations at $B = 4$ T, nominal $T = 2$ K, for pumping powers from 0 to 60 mW. At this field, a distinct absorption peak Z is just starting to resolve out above the rapidly weakening X resonance at the higher n_e values.

name independent of any proposed assignment). It peaks at ≈ 10 meV above the 1s exciton peak X . Peak Z grows as n_e increases, and is stronger in σ^- than in σ^+ .

Peak Z can be seen moving away from the exciton resonance towards higher energy in Fig. 5 for sample *S4*. It resolves out of the wing of the X peak for values of B slightly below 4 T. Figure 8 presents a set of overlaid spectra for sample *S5* under various pumping powers at 4.0 T, showing peak Z just resolved. This figure gives a useful intermediate view between the zero-field spectra of Fig. 4 and the 8 T spectra of Fig. 7.

We have observed magnetoabsorption features similar to Z for many modulation-doped CdTe quantum wells with n_e values ranging up to $\approx 3 \times 10^{11} \text{ cm}^{-2}$. Peak Z is stronger in σ^- polarization than in σ^+ under high fields, that is, it has opposite polarization to the trion resonance. For this reason we initially attributed peak Z (labeled “T1” at the time) to a high-lying electron-spin triplet state of the trion, a *resonance* state.²²

However, the data analysis of Sec. V C will lead us to a severe reinterpretation of peak Z as a *scattering* peak (one might of course suspect this from a simple visual comparison of Fig. 7 and especially Fig. 8 with Fig. 4). This scattering assignment for peak Z will provide a new key to the understanding of the electron concentration dependence of the exciton resonance.

V. SPECTRUM ANALYSIS AND DISCUSSION

A. Zero field spectra

Because of the high optical densities of our MQW samples, Figs. 3 and 4 provide excellent images of the

strengthening of the trion absorption and of the weakening and asymmetric broadening of the exciton absorption with increasing n_e .

We note first, however, that one important known property of the two absorptions seems to be missing here. The splitting $\hbar\omega_X - \hbar\omega_T$ between the two optical excitation thresholds of Eq. (1) should be equal to the energy to dissociate a trion into an exciton and a free electron at the lowest empty electron state, which is at the Fermi level μ in the E_1 conduction subband at $T=0$ K.^{19,27} This splitting is just $E_{bT} + E_F$, where E_{bT} is the trion binding energy in the $n_e \rightarrow 0$ limit (≈ 2.1 meV in 10 nm CdTe wells, Refs. 23 and 27) and E_F is the Fermi energy $= \mu - E_{E1}$ (with E_{E1} the energy of the E_1 subband edge).

In fact, any increase in the exciton-trion splitting seen in Fig. 3 or Fig. 4 is < 0.5 meV, much smaller than the values of the Fermi energy calculated from the formula $E_F = n_e \pi \hbar^2 / m_e$ (e.g., E_F should be 1.4 meV at the estimated maximum electron concentration of $6 \times 10^{10} \text{ cm}^{-2}$ in Fig. 3). We think this means that these samples are so highly disordered by the combined donor and acceptor doping that the Fermi energy E_F is not a meaningful parameter. (A similar regime of constant $\omega_X - \omega_T$ splitting, but occurring at much lower n_e in much higher mobility GaAs quantum wells, has been attributed to disorder effects.²⁸) Also, with the nominal E_F only $\approx 1-2$ meV in our samples, heating to perhaps 10–20 K by the laser beam could be preventing the exciton-trion splitting evolving at the higher pump powers.

We next discuss the spectrum intensities. Although the shape of the absorption spectrum changes dramatically with increasing n_e in Figs. 3 and 4, there is surprisingly little change in its *integrated intensity*, that is, in the total intensity summed over the trion resonance, the exciton resonance, and the high energy wing.

This is shown in Fig. 9, which plots the total absorption intensity integrated over the range of Figs. 3 and 4 for samples S3 and S5, respectively, at the various pump powers. (An exponential base line has been subtracted to simulate the tail of the substrate absorption.)

As explained in Secs. II and V B, we consider that the log (pump power) abscissa in Fig. 9 gives an approximately linear scale of n_e over the ranges shown (of course we have to drop the data for zero pump power). But the proportionality factors and the dark values of n_e are necessarily different for the two samples. The somewhat higher overall optical density for S5 compared to S3 presumably comes from slight differences in the sample parameters, especially well width.

The remarkable stability seen for the integrated intensity in the excitonic region—at most a 5% decrease as n_e increases to nearly 10^{11} cm^{-2} in Fig. 9—is an original, and we believe an important, result of these measurements.

Such a result would have been unexpected in older theories where exciton effects disappear entirely due to phase-space filling and screening.^{18,29,30} But these theories were developed for materials such as GaAs and InGaAs with large exciton Bohr radius a_B and for cases of high electron concentration n_e . Our Fig. 9 is consistent, however, with recent calculations of the optical response^{8,9} that are more appropri-

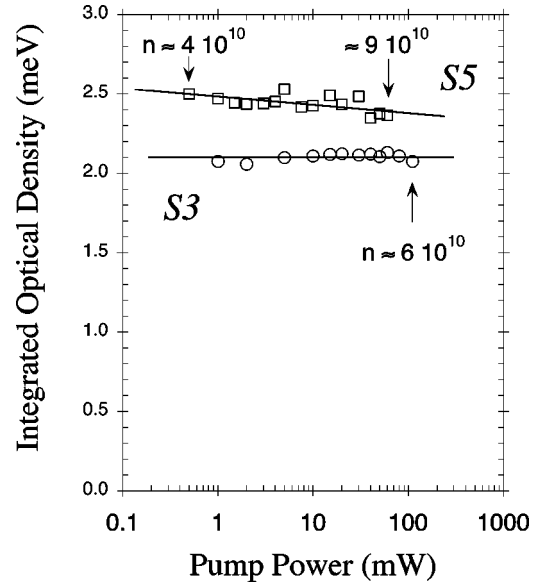


FIG. 9. Optical density $\log_{10}(1/t)$ integrated over the trion and exciton regions of absorption spectra for CdTe MQW samples S3 and S5, in zero field under the pumping powers used in Figs. 3 and 4. Nominal $T=2$ K. Integration is over the full 23 meV wide ranges of Figs. 3 and 4, after subtracting an exponential for substrate absorption. Horizontal line through S3 data and sloping line through S5 data are guides for the eye only. The logarithmic pump power abscissa should give an approximately linear measure of n_e , but different for the two samples. Numbers are estimated n_e values (cm^{-2}).

ate to a dilute electron gas situation $n_e \ll 1/a_B^2$. These recent theories include specifically the essential correlations of three particles (i.e., two electrons, one hole) that generate both an exciton-electron scattering wing and a trion resonance.

Thus, Esser *et al.*⁹ have predicted explicitly that, with increasing n_e , the exciton resonance will transfer oscillator strength to the trion resonance, as well as to the exciton-electron scattering processes, with the total intensity integrated over these three processes falling only very slowly.

The sharing of excitonic oscillator strength is actually obvious to the eye in Figs. 3 and 4 and demonstrated numerically by Fig. 9. Note also that Astakhov *et al.* have found indications of exciton-trion oscillator strength sharing in their zero-field reflectivity spectra of a set of modulation doped ZnSe QW's.³¹

In summary of the present section, with increasing n_e the zero-field optical response evolves progressively to the broad, asymmetric FES-like form. This evolution corresponds (in first order of $n_e a_B^2$) to the trion resonance at threshold $\hbar\omega_T$ with a residual exciton resonance at a second threshold $\hbar\omega_X$ and an exciton-electron scattering wing extending out from $\hbar\omega_X$.

But note that broadening to high energy of the X^- resonance itself, as seen in Fig. 4, requires at least two background electrons: one to bind in the trion and another to scatter the trion. Most recently, Esser *et al.*³² have begun extension of their theory to second order in $n_e a_B^2$ to treat such “quatron” optical excitations (three electrons and one

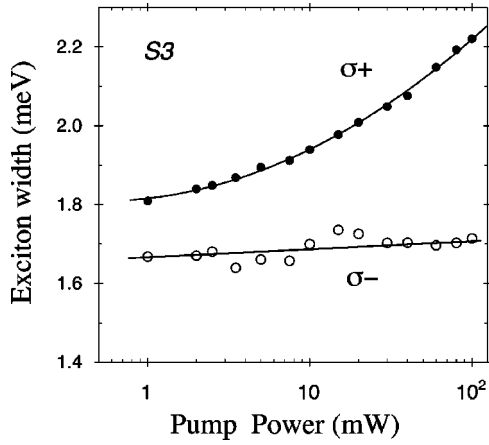


FIG. 10. Width of the Lorentzian fitted to the exciton peak for CdTe MQW sample *S3* in polarizations σ^+ (filled symbols) and σ^- (open symbols) at $B=8$ T, nominal $T=2$ K. $\log(\text{pump power})$ should be an approximately linear scale of n_e . Maximum $n_e \approx 6 \times 10^{10} \text{ cm}^{-2}$. Line and curve through σ^- , σ^+ data, respectively, are guides for the eye.

valence hole). These excitations can be considered as a first stage on the way to the full many-body optical response that gives the traditional Fermi edge singularity at high n_e .

We do not know whether the asymmetric peak seen at the highest n_e for our samples represents a four-body or a many-body optical response. For this reason, we have taken care to call the peak FES-like rather than an FES, everywhere in this paper.

B. Exciton and trion magnetoresonances

In a first analysis of the magnetoabsorption spectra we determined amplitudes, widths, and integrated intensities of absorption peaks X and X^- at $B=8$ T by fitting a Lorentzian function to peak X and a Gaussian function to peak X^- . These two functions give a good fit to the two line shapes, respectively, in both σ^+ and σ^- polarizations, except at the lowest electron concentrations for sample *S3* where the exciton line showed some underlying Gaussian character.

First we discuss the excitonic linewidths. In Fig. 10 we plot the full width of the Lorentzian fitted to the exciton peak as a function of $\log(\text{pump power})$ for sample *S3*. There is a marked broadening of the X peak in σ^+ polarization as n_e increases, with little or no broadening in σ^- . (We are aware that electronic broadening mechanisms could be affected by any laser beam heating, so the data of Fig. 10 may not be absolute, but the σ^- data show there is no strong phonon broadening.)

A symmetric Lorentzian broadening implies a lifetime broadening process, different in nature from the exciton-electron processes identified in zero field. And the σ^+ polarization of the broadening implies that this process is spin dependent.

Polarization-dependent broadening has also been measured in the low-temperature reflectivity spectra of modulation doped CdTe (Ref. 33) and ZnSe (Ref. 31) QW's, as an increase of the exciton's nonradiative damping parameter Γ .

The circular polarization has opposite signs in CdTe where g_e is negative and in ZnSe where g_e is positive. Our results are consistent with inelastic exciton-electron exchange-scattering as proposed by Astakhov *et al.*³¹ Such processes operate on the particular exciton state ($M=-1$ in ZnSe, $M=+1$ in CdTe) whose bound electron has opposite spin to that of the polarized background electrons. Note also that calculations of electron-exciton scattering in zero-field show exchange broadening to be much stronger than direct Coulomb broadening.²¹

The rest of this section and all of Sec. V C will concern the absorption intensities, and especially the reduction of the intensity of the excitonic magnetoresonance X with increasing n_e . We will first show that a large fraction of the lost intensity reappears as the trion magnetoresonance, something that has always seemed obvious but which we evaluate quantitatively here (Sec. V B). But somewhat more than half the missing *polarization-averaged* intensity will then remain unaccounted for, and this will lead us to a new idea: Intensity sharing with a magnetoscattering process, discussed in Sec. V C.

As a way of estimating accurate relative n_e values, following work by Lovisa *et al.*⁴ we believe that the trion absorption intensity in σ^+ at 8 T, low temperature is a good measure of n_e over the range from $n_e=0$ up to $\nu=1$ (which corresponds to $n_e=1.94 \times 10^{11} \text{ cm}^{-2}$ at $B=8$ T). For samples *S3* and *S5* the integrated intensity of X^- in σ^+ polarization showed an almost linear increase when plotted against the logarithm of the pump power (except of course at very low power). Note that this confirms our expectation in Sec. II that n_e should be approximately $\propto \log(\text{pump power})$, based on the properties of a tunneling-limited charge transfer process.

So the σ^+ trion intensity $I_T^{\sigma^+}$ provides a useful scale for plotting the excitonic properties although, since oscillator strength depends on structure parameters, especially the QW width, the scaling factor may vary from sample to sample. Also, for the present samples showing significant depolarization, we use the total trion intensity $I_T^{\text{tot}} = I_T^{\sigma^+} + I_T^{\sigma^-}$ as a scale of n_e .

Thus in Fig. 11 we plot the integrated intensities of the X resonance $I_X^{\sigma^+}$ and $I_X^{\sigma^-}$ against I_T^{tot} for samples *S3* and *S5*. We use a double x , double y scale in this figure because the zero-field studies (Fig. 9) showed that sample *S5* has higher optical density than sample *S3*: the x and y scales for *S5* are each set to 15/16 times the x and y scales for *S3*, an arbitrary adjustment that brings the optical densities for the two samples into approximate coincidence. One can then see that the σ^+ and σ^- intensity data for *S5* overlap and prolong the σ^+ and σ^- intensity data for sample *S3*.

This implies that the relation between the intensities of the X and X^- peaks, as n_e varies, is a well-defined law for a given high field B and a given set of QW parameters.

The main feature seen in Fig. 11 is a strong decrease of intensity for the exciton resonance peak in *both* polarizations with increasing n_e . The decrease appears to be a little faster in σ^+ than in σ^- , but not much. [Note that one can be misled by spectra obtained at n_e values where $I_X^{\sigma^+}$ is nearing

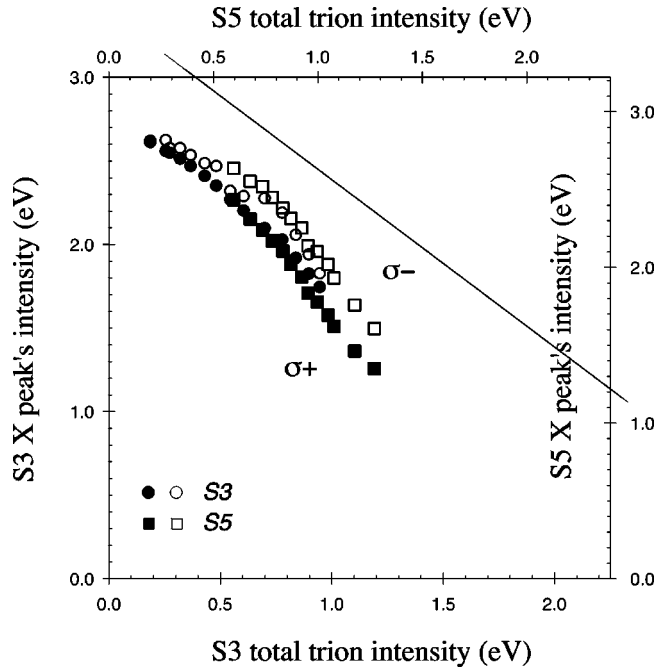


FIG. 11. Integrated optical densities at $B=8$ T, nominal $T=2$ K, and various pump powers for peak X in CdTe MQW samples S3 (circles) and S5 (squares) in polarizations σ^+ (filled symbols) and σ^- (open symbols). The x, y scales of S3 and S5 were adjusted proportionally to bring their data points into approximate coincidence. Abscissas are I_T^{tot} = integrated optical density of the trion peak in the same sample summed over σ^+ and σ^- . This abscissa should be directly proportional to n_e (maximum n_e is $\approx 0.9 \times 10^{11} \text{ cm}^{-2}$, equivalent to $\nu \approx 0.46$). Reference straight line has slope -1 for both samples.

zero on its intensity curve and the anisotropy of the residual intensities $(I_X^{\sigma^-} - I_X^{\sigma^+}) / (I_X^{\sigma^-} + I_X^{\sigma^+})$ becomes very large.]

There is no convenient theory of excitonic intensities relevant to the case of CdTe quantum wells at 8 T. We have an intermediate field situation, combined with fairly low n_e , see Ref. 34 listing relative length scales for magnetic length l_B , excitonic radius, and interelectronic distance. High-field approximations exist, but high field means $l_B \ll$ excitonic radius, or combined electron and hole Landau energy \gg exciton binding energy $E_{bX}=16$ meV, whereas we have $\frac{1}{2}(\hbar\omega_{ce} + \hbar\omega_{ch})=6$ meV only (which is why the exciton's energy position is quadratic in B still at 8 T in Fig. 5, not linear in B). We will reexamine two mechanisms—screening and phase-space filling—that are frequently invoked to explain the attenuation of QW excitons in the presence of free electrons. We will then discuss how intensity sharing, discussed above for the zero-field case (Sec. V A), is modified by the magnetic field.

We first mention screening.¹⁸ Qualitatively, screening of the electron-hole interaction by a sea of $m=+1/2$ spin polarized electrons could well produce the reduction of intensity seen in both polarizations but somewhat stronger for the σ^+ exciton if Pauli exclusion effects are considered (the σ^+ exciton is made with an $m=-1/2$ electron bound to an $m=+3/2$ hole). We note that Lemaître *et al.*³⁵ have postulated very strong screening to explain the energy positions of the

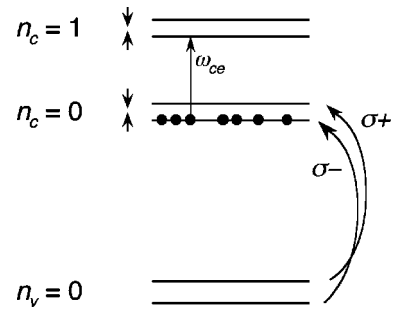


FIG. 12. Creation of σ^+ and σ^- excitons and trions is shown in very high magnetic field, where the exciton and trion are made mainly of electron-hole pair excitations in $n=0$ conduction- and valence-band Landau levels. Background electrons are shown polarized spin up ($m=+1/2$) at $\nu < 1$. One expects weakening of the σ^- exciton oscillator strength by phase-space filling, but the present work seriously questions this (and therefore the usefulness of drawings like this one). One also expects stealing of σ^+ exciton oscillator strength by σ^+ trion creation, which is confirmed by the present work. Cyclotron excitation of a background electron is shown for discussion in Sec. V C.

ladder of transitions seen for n -type CdMnTe wells with $n_e \approx 2 \times 10^{11} \text{ cm}^{-2}$ (rather higher than our own n_e values). Also, screening by 2D holes was invoked as a major influence on the exciton intensity in p -type CdMnTe quantum wells at zero or very small fields ($B < 1$ T).¹²

But it seems to us now that this may be assigning screening too important a role. Screening (a mean-field concept) does not appear in the recent theory of the optical response for low n_e which, by emphasizing few-particle correlations, gives an excellent explanation of amongst other things the trion absorption.⁹ The theory is for zero-field only at present, but an 8 T field will tend to reduce if anything the effects of screening, depending on ν .³⁰ Moreover, in two-dimensional systems, screening is generally considered to be less important than phase-space filling.

So we next consider, referring to Fig. 12, the possible effect of phase-space filling, in particular for the σ^- exciton, which consists of an $m=+1/2$ photoelectron with an $m=-3/2$ photohole.

In high magnetic field, the excitations illustrated in Fig. 12 that create the lowest electron-hole pair state (Landau state $n_c=n_v=0$), have a large weight in the exciton's wave function. So as ν increases from zero towards 1, filling the lowest spin sublevel ($m=+1/2$) of the $n=0$ conduction level with electrons, one expects the σ^- exciton to weaken. In very high field, where one would have a nearly pure $n=0$ "magnetoexciton," the intensity I_X would be proportional to $(1-\nu)$ or to $1-n_e l_B^2$ (where l_B is the magnetic length).

This has been our model for the weakening of peak X in σ^- till now.²²⁻²⁴ But it ignores that 8 T is not a very high field for CdTe (and that we do not have the correspondingly very high n_e that would be needed to approach $\nu=1$ at very high fields; see numbers in Ref. 34). At 8 T, the exciton wave function is made from many Landau levels, not just the $n=0$ levels. Now, for zero field there is a simple formula for the effect of space-face filling on the exciton intensity:

$$I_X(n_e) = \frac{1}{(1 + n_e \pi a_B^2/2)} I_X(0) \quad (2)$$

(see, e.g., Ref. 29). This gives an upper limit on the strength of phase-space filling at $B=0$, because it assumes the wave function does not adjust to the filling.

Equation (2) predicts $<7\%$ intensity loss at $n_e = 10^{11} \text{ cm}^{-2}$ in a CdTe QW. Furthermore, comparing the very high-field formula $I_X \propto 1 - n_e l_B^2$ with a low n_e approximation to Eq. (2), $I_X \propto 1 - n_e \pi a_B^2/2$, we expect the effect of phase-space filling to decrease continuously on progressing from zero field to very high field *at constant* n_e .

Also (neglecting the small electron spin depolarization), phase-space filling cannot explain any part of the even faster loss of intensity for the peak associated with the σ^+ exciton made with an $m = -1/2$ electron and an $m = +3/2$ hole, since the $m = -1/2$ conduction sublevel remains empty until $\nu = 1$ (that is, until n_e reaches $1.94 \times 10^{11} \text{ cm}^{-2}$ at 8 T).

In any case, as mentioned in Sec. V A, the recent theory for zero-field indicates that, for $n_e a_B^2 \ll 1$, phase-space filling affects the exciton intensity very much less than intensity sharing, which we now consider.

In fact, since the discovery of the trion, our model for the carrier-induced weakening of the σ^+ exciton resonance in CdTe QW's has always been "intensity stealing" by (or sharing of intensity to) the trion resonance.²²⁻²⁴ The idea was that excitonic oscillator strength at $\hbar\omega_X$ just gets shifted down in energy a little to become trion oscillator strength at $\hbar\omega_T$ as the 2D space fills with electrons. This has seemed self-evident if one considers the trion X^- as a neutral exciton core with a more loosely bound "outer" electron, and it is now supported by the recent theoretical work.

Polarization-dependent intensity sharing between exciton and trion has also been invoked to explain spectra obtained at nearly zero field in semimagnetic $\text{Cd}_{1-x}\text{Mn}_x\text{Te}$ quantum wells.^{12,36} Therefore, we continue to propose intensity stealing by the trion as a real and major cause of loss of σ^+ exciton intensity with increasing n_e in a magnetic field.

There is nevertheless a small quantitative problem. The slope of any line that one could draw through the intensity data for the σ^+ exciton peak in Fig. 11 is significantly steeper than 1 (compare with the reference line). So intensity sharing with the trion is not everything, even in σ^+ . And in σ^- , where there is no trion (neglecting spin depolarization), we need a new explanation for the attenuation of peak X .

So is intensity lost by the excitonic resonance in σ^- with increasing n_e transferred elsewhere? We address this question in Sec. V C and the answer does indeed appear to be yes.

C. Magnetoscatting

Figure 13 gives (at top) the total absorption intensity for sample S5 at the various pumping powers. The intensity is integrated numerically over a wider spectrum range than just the X and X^- resonances, between the two "static" points a and c marked in Fig. 7. This extended range includes the broad peak we have labeled Z in Fig. 7.

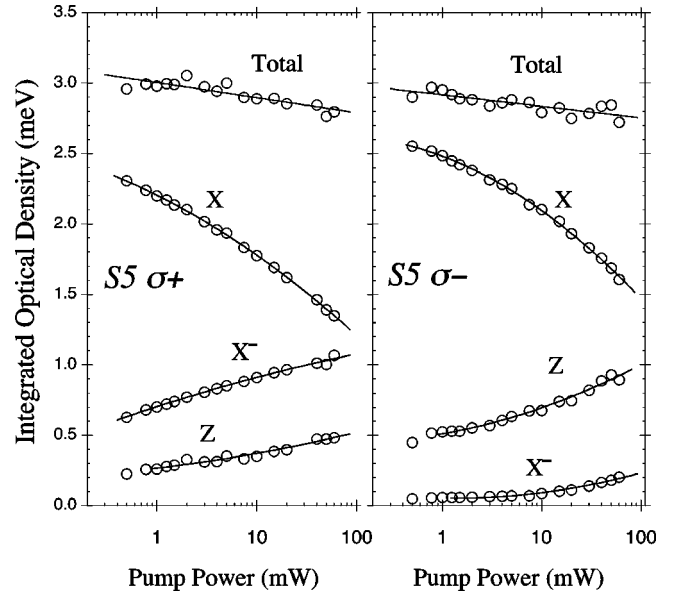


FIG. 13. Optical density $\log_{10}(1/t)$ at $B=8$ T for trion and exciton resonances and absorption band Z for sample S5 in σ^+ (at left) and σ^- (at right). In both polarizations, "Total" is numerical integral between points 1603.0 meV and 1628.1 meV, marked by arrows a and c in Fig. 7. "Z" is partial numerical integral from point b to point c in Fig. 7 for σ^- , and equivalent range for σ^+ . "X" is intensity of Lorentzian fitted to the exciton resonance, and "X-" is intensity of Gaussian fitted to trion resonance. Abscissa should be an approximately linear scale of n_e (maximum n_e is $\approx 0.9 \times 10^{11} \text{ cm}^{-2}$, equivalent to $\nu \approx 0.46$). Least-squares fits (linear fits for total integrals, second-order polynomials for partial integrals) are plotted through data as guides for the eye.

Remarkably, the total integrated intensity then decreases only 6% or 7% over the range of n_e available with sample S5 (which goes from perhaps 4×10^{10} up to $\approx 9 \times 10^{10} \text{ cm}^{-2}$). This is true in both polarizations; see Fig. 13 (left and right).

Note that the total intensity data in Fig. 13 can shift up or down depending on the base line chosen for the integrations (we subtract an exponential base line, slightly different for the σ^- spectra and σ^+ spectra, that approximates the underlying absorption tail of the CdZnTe substrate), so the absolute precision is perhaps only 5% or 10%. But any intensity shift from this cause will be the same for all data points in one graph.

Note also that, comparing Fig. 13 with the zero-field integrations of Fig. 9, we find only $\approx 20\%$ magnetic-field induced enhancement of the total absorption intensity for sample S5. This confirms that we are far from the very high-field limit where I_X becomes linear in B .

Figure 13 also gives the partial intensities for the three spectrum components X^- , X , and Z for each polarization. We split off the integration range of Z by choosing (in each polarization) a point b that appeared to be the energy threshold of Z (see Fig. 7). Splitting between X^- and X was more difficult because the two resonances overlap considerably. So, as in Fig. 11, we have plotted the intensities of the fitted Lorentzian peak for X and the fitted Gaussian peak for X^- . (Partly because of the base line and fitting uncertainties, the

X , X^- , and Z intensities in Fig. 13 do not add up exactly to the numerically integrated overall spectrum intensity “Total.”)

Figure 13 obviously recalls Fig. 9, which showed near stability of the sum of trion, exciton, and electron-exciton scattering states with increasing n_e in zero field and comparison of Fig. 7 (8 T spectra) and Fig. 8 (4 T spectra) with Fig. 4 (zero field spectra of the same sample) shows that peak Z appears in the energy region of the electron-exciton scattering wing of the zero-field case. Also, the X - Z splitting of ≈ 10 meV corresponds approximately to the electron cyclotron energy $\hbar\omega_c$ of 8.9 meV at 8 T. All this suggests that peak Z corresponds to the electron-exciton scattering states, but transformed by a magnetic-field induced quantization of the free-electron momentum.

Which is forcing us to abandon finally our early attribution of peak Z to a resonance state, an electron spin triplet state of X^- with one of the bound electrons on the $n=1$ Landau level.²² Following a suggestion made by Kheng *et al.*³⁷, we now assign peak Z to the combined exciton and cyclotron-scattering process discovered by Yakovlev *et al.*¹⁰ This process can be written as

$$\hbar\omega + e_0 \rightarrow X + e_1, \quad (3)$$

where e_0 and e_1 mean an electron on Landau levels $n=0$ and $n=1$, respectively (the cyclotron excitation $0 \rightarrow 1$ is shown in Fig. 12). As explained in Ref. 10, this is just the magnetically quantized version of the scattering process that broadens the exciton resonance asymmetrically in zero field,

There are nevertheless some problems with this assignment. The detailed theory¹⁰ given for the exciton-electron scattering process incorporates the requirement that the exciton must recoil to compensate the electron's momentum change in Eq. (3). With respect to the exciton resonance at $\hbar\omega_X$, the maximum of absorption should occur at

$$\hbar\omega = \hbar\omega_X + \hbar\omega_c(1 + m_e/M_X), \quad (4)$$

where $M_X = m_e + m_h$ is the exciton mass.

With $m_e = 0.105m_0$ in 10 nm CdTe quantum wells, the bare cyclotron energy $\hbar\omega_c$ is 1.11 meV/T. Plausible values for the in-plane hole mass m_h in our highly strained wells range from a calculated band-mixed mass of $0.25m_0$ to the diagonal (no-mixing) mass of $0.18m_0$. With these mass values the momentum conservation formula (4) predicts that the scattering peak should separate from the X resonance peak with a slope in the range from 1.44 to 1.52 meV/T.

In fact, the slope of the energy separation $E_Z - E_X$ is 1.13 meV/T for sample *S5* when measured at the lowest n_e value where accurate measurement is possible. This number seems too low, being essentially the bare cyclotron energy, but it corresponds to the value first measured by Yakovlev *et al.* in CdTe QW's (1.14 meV/T), also at quite low n_e .¹⁰

We find that the slope of $E_Z - E_X$ increases considerably with increasing n_e . It is 1.37 meV/T for sample *S5* at its maximum n_e and 1.51 meV/T for sample *S4* in the dark ($n_e = 1.1 \times 10^{11} \text{ cm}^{-2}$). These slope values fit better with Eq. (4) but, whereas the difference $E_Z - E_X$ extrapolates accurately to zero at $B=0$ for the lowest n_e values, it moves

progressively to negative energies (by about -2 meV over the n_e range of sample *S5*), and this does not fit well with Eq. (4). Similar numbers have been reported recently by Kochereshko *et al.*³⁸

We do not understand these variations, and a detailed description of the properties of peak Z is beyond the scope of the present paper. Perhaps collective electron excitation effects (magnetoplasmons) need consideration at higher n_e values. In fact, as observed for a variety of CdTe QW's, our Z peak—or rather “ Z band”—appears to have a substructure, different in the two polarizations, and changing with B and n_e . Moreover there is a series of such absorption bands, attributed by Yakovlev *et al.*¹⁰ to promotion of an electron to Landau levels $n=1,2,\dots$

There is an alternative explanation of absorption features having the characteristics of band Z , in the more traditional description much used in discussion of modulation-doped GaAs QW's. That is the very high field description, where successive absorption peaks are assigned to the hierarchy of optically allowed magnetoexciton levels $n=0,1,2,\dots$, that is, to electron hole pairs in the $n_c = n_v = n$ conduction and valence Landau levels. Band Z could be assigned to the $n=1$ magnetoexciton, situated at distance $\hbar\omega_c(1 + m_e/m_h)$ —hardly distinguishable from $\hbar\omega_c(1 + m_e/M_X)$ —above the ground $n=0$ magnetoexciton.

In fact, exactly this interpretation has been given most recently by Fromer *et al.*³⁹ for a broad peak, very similar to the CdTe Z band, seen in the σ^+ absorption spectrum of GaAs MQW's with $n_e = 2 \times 10^{11} \text{ cm}^{-2}$. They assign this to the $n=1$ magnetoexciton creation transition, broadened by a magnetoplasmon effect.

We do not think such a description appropriate for CdTe QW's at 8 T and $n_e = 10^{11} \text{ cm}^{-2}$ (see also Ref. 25). Our data all favor a “low B , low n_e ” description. We mean by this that peak Z corresponds to a $1s$ exciton (i.e., electron and hole interacting much more strongly with each other than with the magnetic field), and that this exciton is almost unaffected by screening or phase-space filling but is scattered to higher k -vector states. It appears that in these circumstances, the exciton's oscillator strength is essentially preserved, that is, merely shifted to higher energy.

If we accept that band Z corresponds to exciton-electron scattering, Fig. 13 provides a fairly complete resolution of the difficulties encountered in Sec. V B.

(1) In σ^- , one can see clearly the X resonance sharing intensity with scattering band Z and with the weak (depolarization related) trion resonance.

(2) In σ^+ , one can see the X resonance sharing intensity with the X^- resonance, as already discussed in Sec. V B, as well as with a weak Z scattering band.

(3) There is only a relatively small overall loss of intensity ($< 10\%$), in either polarization, just as in zero field.

It seems therefore that there is no fundamental difference between $B=8$ T and zero field: Intensity lost by the excitonic resonance is shared out to (stolen by) the trion resonance and electron-exciton scattering. However, in a magnetic field the intensity sharing is *circularly polarized*. And this has allowed us to separate the two components of the sharing.

So finally, for explaining the intensity variation of the excitonic absorption resonance in our samples, intensity sharing appears to be everything, or almost. With $n_e \ll 1/a_B^2$, screening and phase space filling need not be invoked except perhaps to explain the relatively small losses of *total* oscillator strength.

As concerns experiments where B is swept at fixed n_e , we would now attribute the emergence and then progressive strengthening of the exciton resonance with increasing field B to a progressive decrease of the efficiency of the magnetoscattering progress as the cyclotron energy $\hbar\omega_{ce} = eB/m_e$ increases. In this view, filling factor ν plays no special role and the emergence of the resolved resonance near $\nu=1$ is perhaps accidental.

The trion has in a sense simpler magneto-optical properties than the exciton at 8 T. The trion resonance, seen essentially in σ^+ , remains Gaussian in high field at all n_e studied here, and from Ref. 4 we know that in CdTe QW's at 8 T its intensity increases linearly with n_e up to $\nu=1$. Apparently, at least at $B \approx 8$ T, the trion is rather impervious to possible scattering or screening effects in this range, because such effects would be second order in the electron concentration or simply because the trion's negative charge repels electrons. And any phase-space filling cannot affect the σ^+ trion for $\nu < 1$ (see Fig. 12).

It is known that from $\nu=1$ to $\nu=2$ (beyond the range of our Fig. 11), the σ^+ trion peak loses intensity and disappears.⁴ Referring to Fig. 12, it would seem blatant that this intensity loss is due to phase-space filling by spin-down electrons on the upper sublevel blocking out the $n_c = n_v = 0$ Landau-level excitations in σ^+ . This has been our model previously (see especially Ref. 4), but the present work makes us much less certain that phase-space filling can explain any optical property of CdTe QW's at concentrations $n_e \approx 10^{11} \text{ cm}^{-2}$.

At these n_e , the fields B corresponding to $\nu=1-2$ are not high fields and the trion's wave function involves mixing of many Landau levels.⁴⁰ So the extinction of the trion resonance at precisely $\nu=2$ with increasing n_e (and its emergence at $\nu=2$ with increasing B) remains a mystery.

VI. CONCLUSION

In fact, it is hard to extract accurately the intensities of the different spectrum components even for these thick MQW samples. There are various anomalies in our results. For example, the model of intensity sharing linear in n_e implies that the intensity of the X resonance should decrease linearly initially, whereas the data of Fig. 11 have a definite curvature near the origin (zero of trion intensity) for the lower concentration sample S3. At higher n_e , one does of course expect a downward curvature, because effects second order in n_e ("quatron" effects) or higher must start up, as demonstrated by the evolution to the FES-like form in zero field. But our measurement accuracy was not good enough to study this properly.

To get a really good intensity law for X at 8 T field, we would need to be able to vary n_e all the way from 0 to about $2 \times 10^{11} \text{ cm}^{-2}$ in a single sample. Nevertheless, the samples

studied here have shown more clearly than in previous work how the exciton peak attenuates and broadens and how the trion peak grows, both in zero field and under magnetic field.

Although the attenuation of the excitonic resonance with increasing n_e looks dramatic, very little oscillator strength is actually lost. A large part of the intensity is just shifted up in energy to optical transitions that create excitons with *non zero momentum*, simultaneous with electron scattering. Another large part of the oscillator strength is shifted down in energy to the trion creation transitions. Less than 10% of the excitonic oscillator strength is unaccounted for.

These results show that, at n_e of order 10^{11} cm^{-2} in CdTe quantum wells, there is hardly any change of the exciton wave function, at least in the traditional sense of effects of phase-space filling and screening.⁴¹ And, moreover, that the exciton wave function is hardly modified by a medium-sized field like 8 T. This low n_e , low B description of the excitonic effects is contrary to models frequently used to interpret optical and magneto-optical spectra for other QW systems, but we believe it is valid here.

Further work is needed to unravel more accurately the different contributions of the processes involved in intensity sharing/stealing, as well as the possible contributions of phase-space filling and screening, particularly at higher n_e where the latter two effects must inevitably become significant.

ACKNOWLEDGMENTS

This paper draws very much on the accumulated work of the Grenoble II-VI semiconductor research group of the CEA, the CNRS, and Joseph Fourier University. Concerning previous optical work on X^- and X , the pronoun "we" as used in the paper is often meant to include other group members, especially V. Huard, K. Kheng, S. Lovisa, and the late Yves Merle d'Aubigné. We thank J. Cibert for valuable discussions during the manuscript writing. Also, R.T.C. wishes to acknowledge V.P. Kochereshko's tireless efforts to convince him he was in error about many things, some of which errors have hopefully been resolved in this paper.

APPENDIX IDENTIFICATION OF LS AND HS ELECTRON-ACCEPTOR EMISSION SPECTRA

The electrons participating in the two series of electron-acceptor recombination peaks called HS and LS in Sec. III must be situated in the quantum wells, as barrier electrons would give peaks at about 40 meV higher energy. But the location of the acceptors is less obvious. Because the valence-band offset is small, acceptor levels lie at similar absolute energies in the wells and in the barriers.

To interpret the emission of Fig. 2, we take the quantum well exciton peak (X) as reference of energy. The higher series and lower series zero-phonon peaks lie at $\Delta = 28$ and $\Delta = 37$ meV below X (in zero magnetic field). If the acceptor were in the quantum well, the parameter Δ would be just $E_{bA} - E_{bX}$, where E_{bA} and E_{bX} are the acceptor and exciton binding energies respectively.

Thus, with $E_{bX} = 16$ meV for these wells, the acceptor

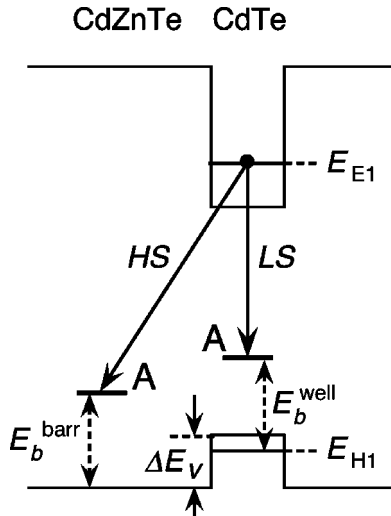


FIG. 14. Energy-level diagram for recombination of QW E_1 subband electrons with holes on QW acceptor levels A_{QW} (the lower series LS) and on barrier acceptor levels A_{barrier} (higher series HS).

levels involved in the HS and LS recombinations would have to have binding energies 44 and 53 meV, respectively. The first number (44 meV) looks wrong, but 53 meV is close to $E_{bA} = 55$ meV measured for nitrogen acceptors in thick CdTe layers.^{42,43} It is also close to a value of $E_{bA} = 52$ meV measured for 13 nm wide $\text{Cd}_{0.96}\text{Zn}_{0.04}\text{Te}$ quantum wells doped with nitrogen.⁴⁴ (The anomalous *decrease* of E_{bA} in a quantum well comes from strong strain effects on a heavy hole acceptor level.⁴⁴)

So we attribute the lower energy series LS to recombina-

tion of quantum well electrons with nitrogen acceptors situated within the quantum well. The very high intensity of this emission in Fig. 2 implies there has been large segregation or diffusion of nitrogen into the wells.

The origin of the higher series, which is less intense than the lower series, is less obvious. However, identical circular polarizations observed for the LS and HS emissions at $B = 8$ T show that they both involve heavy hole acceptor states. We suggest that the HS emission corresponds to indirect recombination of quantum well electrons with acceptors situated in the barriers near the well edge.

In this interpretation, as shown in Fig. 14, the HS-LS energy difference $\Delta E = 9$ meV is just the difference between the absolute energies of well and barrier acceptor levels. It is made up of the binding-energy difference between quantum well and barrier acceptors plus the difference between the 2D QW and the 3D barrier reference levels:

$$\Delta E = (E_{bA}^{\text{well}} - E_{bA}^{\text{barrier}}) + (\Delta E_v - \Delta E_{H1}). \quad (\text{A1})$$

In Eq. (A1), binding energies E_{bA}^{well} and E_{bA}^{barrier} are measured with respect to the H_1 subband edge in the quantum well and to the 3D valence band edge in the CdZnTe barrier, respectively; ΔE_v is the valence-band offset and ΔE_{H1} is the confinement-induced shift of the QW H_1 subband with respect to the 3D CdTe valence band; see Fig. 14.

With $E_{bA}^{\text{well}} = 53$ meV, $E_{bA}^{\text{barrier}} = 55$ meV, $E_{H1} = 3$ meV, and taking $\Delta_v = 1.3x = 17.5$ meV for the CdTe/ $\text{Cd}_{1-x}\text{Zn}_x\text{Te}$ heavy hole valence-band offset,¹⁵ we expect $\Delta E = 12.5$ meV close enough to the measured separation of 9 meV between the HS and LS peaks to justify our attribution of the HS emission to recombination of QW electrons with holes on barrier acceptors.

¹C. Delalande, G. Bastard, J. Orgonasi, J.A. Brum, H.W. Liu, M. Voos, G. Weimann, and W. Schlapp, Phys. Rev. Lett. **59**, 2690 (1987).

²G. Finkelstein, H. Shtrikman, and I. Bar-Joseph, Phys. Rev. Lett. **74**, 976 (1995).

³A.J. Shields, M. Pepper, D.A. Ritchie, M.Y. Simmons, and G.A.C. Jones, Phys. Rev. B **51**, 18 049 (1995).

⁴S. Lovisa, R.T. Cox, N. Magnea, and K. Saminadayar, Phys. Rev. B **56**, 12 787 (1997).

⁵R.B. Miller, T. Baron, R.T. Cox, and K. Saminadayar, J. Cryst. Growth **184/185**, 822 (1998).

⁶B. Stébé, E. Feddi, A. Ainane, and F. Dujardin, Phys. Rev. B **58**, 9926 (1998).

⁷F.X. Bronold, Phys. Rev. B **61**, 12 620 (2000).

⁸R.A. Suris, V.P. Kochereshko, G.V. Astakhov, D.R. Yakovlev, W. Ossau, J. Nürnberger, W. Faschinger, G. Landwehr, T. Wojtowicz, G. Karczewski, and J. Kossut, Phys. Status Solidi B **227**, 343 (2001).

⁹A. Esser, R. Zimmermann, and E. Runge, Phys. Status Solidi B **227**, 317 (2001) Note that the numerical calculations reported in this paper were limited to 1D quantum wires to get reasonable computing times, but they demonstrated general principles ex-

pected to be valid for a 2D quantum well.

¹⁰D.R. Yakovlev, V.P. Kochereshko, R.A. Suris, H. Schenk, W. Ossau, A. Waag, G. Landwehr, P.C.M. Christianen, and J.C. Maan, Phys. Rev. Lett. **79**, 3974 (1997).

¹¹T. Baron, F. Kany, K. Saminadayar, N. Magnea, and R.T. Cox, Appl. Phys. Lett. **70**, 2963 (1997).

¹²P. Kossacki, J. Cibert, D. Ferrand, Y. Merle d'Aubigné, A. Arnoult, A. Wasiela, S. Tatarenko, and J.A. Gaj, Phys. Rev. B **60**, 16 018 (1999).

¹³T. Baron, K. Saminadayar, and N. Magnea, Appl. Phys. Lett. **67**, 2972 (1995).

¹⁴E.F. Schubert and K. Ploog, Phys. Rev. B **29**, 4562 (1984).

¹⁵P. Peyla, Y. Merle d'Aubigné, A. Wasiela, R. Romestain, H. Mariette, M.D. Sturge, N. Magnea, and H. Tuffigo, Phys. Rev. B **46**, 1557 (1992).

¹⁶M. Combescot and P. Nozières, J. Phys. (Paris) **32**, 913 (1971).

¹⁷M. Combescot and C. Tanguy, Phys. Rev. B **50**, 11 484 (1994).

¹⁸S. SchmittRink, D.S. Chemla, and D.A.B. Miller, Adv. Phys. **38**, 89 (1989).

¹⁹P. Hawrylak, Phys. Rev. B **44**, 3821 (1991).

²⁰J.A. Brum and P. Hawrylak, Comments Condens. Matter Phys. **18**, 135 (1997).

- ²¹G. Ramon, A. Mann, and E. Cohen, Phys. Rev. B **67**, 045323 (2003).
- ²²R. T. Cox, K. Kheng, K. Saminadayar, T. Baron, and S. Tatarenko, in *High Magnetic Fields in the Physics of Semiconductors*, edited by D. Heimann (World Scientific, Singapore, 1995), p. 394.
- ²³K. Kheng, R.T. Cox, Y. Merle d'Aubigné, Franck Bassani, K. Saminadayar, and S. Tatarenko, Phys. Rev. Lett. **71**, 1752 (1993).
- ²⁴R.T. Cox, V. Huard, K. Kheng, S. Lovisa, R.B. Miller, K. Saminadayar, A. Arnoult, J. Cibert, S. Tatarenko, and M. Potemski, Acta Phys. Pol. **94**, 99 (1998).
- ²⁵The disappearance of the $2s$ exciton peak *in place* at quite small n_e values has an interesting general implication, given that magnetoabsorption peaks seen in its energy range for modulation doped quantum wells with high n_e are often assigned to the $2s$ exciton or $n=1$ magnetoexciton. It is hard to understand how the $2s$ resonance could reappear at higher n_e . This is another point in favor of a magnetoscattering interpretation of such peaks.
- ²⁶T. Wojtowicz, M. Kutrowski, G. Karczewski, J. Kossut, F.J. Teran, and M. Potemski, Phys. Rev. B **59**, 10 437 (1999).
- ²⁷V. Huard, R.T. Cox, K. Saminadayar, A. Arnoult, and S. Tatarenko, Phys. Rev. Lett. **84**, 187 (2000).
- ²⁸G. Yusa, H. Shtrikman, and I. Bar-Joseph, Phys. Rev. B **62**, 15 390 (2000).
- ²⁹Daming Huang, Jen-Inn Chyi, and H. Morko, Phys. Rev. B **42**, 5147 (1990).
- ³⁰G.E.W. Bauer, Phys. Rev. B **45**, 9153 (1992).
- ³¹G.V. Astakhov, V.P. Kochereshko, D.R. Yakovlev, W. Ossau, J. Nürnberg, W. Faschinger, G. Landwehr, T. Wojtowicz, G. Karczewski, and J. Kossut, Phys. Rev. B **65**, 115310 (2002).
- ³²A. Esser, M. A. Dupertuis, E. Runge, and R. Zimmermann, in *Physics of Semiconductors 2002, Proceedings of the 26th International Conference, Edinburgh 2002*, edited by A. R. Long and J. H. Davies, IOP Conf. Proc. No. 171 (IOP Publishing, Bristol, 2003), p. R4.2.
- ³³V.P. Kochereshko, A.V. Platonov, F. Bassani, and R.T. Cox, Superlattices Microstruct. **24**, 269 (1998)
- ³⁴Some useful numbers: The 3D Bohr radius a_B is 7 nm for an exciton in CdTe. In our quasi-2D 10 nm quantum wells, the in-plane exciton radius is perhaps half way between this value and the 2D Bohr radius $a_B/2=3.5$ nm. At our maximum field of 8 T, the magnetic length $l_B=\sqrt{\hbar}/eB$ (which is the radius of the Gaussian $m=0$ wave function of an electron in the symmetric representation) is still relatively large: $l_B=9.1$ nm at 8 T. Our data concern concentrations n_e ranging up to $\approx 10^{11}$ cm $^{-2}$. At $n_e=1\times 10^{11}$ cm $^{-2}$ (mean separation between electrons $1/\sqrt{n_e}=32$ nm), the Landau level filling factor $\nu=0.52$ at 8 T.
- ³⁵A. Lemaître, C. Testelin, C. Rigaux, T. Wojtowicz, and G. Karczewski, Phys. Rev. B **62**, 5059 (2000).
- ³⁶T. Brunhes, R. André, A. Arnoult, J. Cibert, and A. Wasiela, Phys. Rev. B **60**, 11 568 (1999).
- ³⁷K. Kheng, K. Saminadayar, and N. Magnea, Physica E (Amsterdam) **2**, 256 (1998).
- ³⁸V.P. Kochereshko, M. Kutrowski, D.A. Andronikov, T. Wojtowicz, G. Karczewski, and J. Kossut, Phys. Status Solidi C **0**, 1463 (2003).
- ³⁹N.A. Fromer, C. Schüller, C.W. Lai, D.S. Chemla, I.E. Perakis, D. Driscoll, and A.C. Gossard, Phys. Rev. B **66**, 205314 (2002).
- ⁴⁰Moreover, in *infinite* magnetic field (no Landau level mixing) and with equal $e-e$ and $e-h$ interactions, the electron-spin singlet trion X^- which is such a major feature of real-world spectra would not exist! See, e.g., J.J. Palacios, D. Yoshioka, and A.H. MacDonald, Phys. Rev. B **54**, 2296 (1996).
- ⁴¹A scattered exciton's wave function is nevertheless modified in the three particle theory when it is properly antisymmetrized to the scattered electron's wave function, but there is no marked loss of total oscillator strength: A. Esser (private communication).
- ⁴²K.A. Dhese, P. Devine, D.E. Ashenford, J.E. Nicholls, C.G. Scott, D. Sands, and B. Lunn, J. Appl. Phys. **76**, 5423 (1994).
- ⁴³T. Baron, K. Saminadayar, and N. Magnea, J. Appl. Phys. **83**, 1354 (1998).
- ⁴⁴Q.X. Zhao, T. Baron, K. Saminadayar, and N. Magnea, J. Appl. Phys. **79**, 2070 (1996).